RSC Advances

PAPER

View Article Online
View Journal | View Issue

Cite this: *RSC Adv.*, 2020, **10**, 23936

Effective photocatalytic degradation and physical adsorption of methylene blue using cellulose/GO/TiO_2 hydrogels†

Yian Chen,[a] Zhouyang Xiang,[a] Desheng Wang,[b] Jian Kang*[b] and Haisong Qi*[a]

Received 21st May 2020
Accepted 17th June 2020

DOI: 10.1039/d0ra04509h

rsc.li/rsc-advances

Environmentally friendly cellulose/GO/TiO_2 hydrogel photocatalyst has been successfully fabricated *via* a green, simple, and one-step method and evaluated as the photocatalyst and adsorbent for the removal of methylene blue (MB). The XRD and FTIR analysis suggested the strong interaction among cellulose, GO and TiO_2, resulting from the formation of hydrogen bonds. Due to the unique porous structure of cellulose hydrogel and introduction of GO, the cellulose/GO/TiO_2 hydrogel showed superior (degradation ratio ~ 93%) and reproducible (no significant change during the ten consecutive cycles) performance in the removal of MB under UV light. Consequently, the prepared cellulose/GO/TiO_2 hydrogel can be applied as an eco-friendly, high-performance, reproducible, and stable photocatalyst and adsorbent for the removal of MB. This green hydrogel is a promising candidate for dye wastewater treatment. Moreover, this work is expected to extend the scope of bio-templated synthesis of other nanomaterials for various applications.

1. Introduction

Dye wastewater is mainly from textile, leather, paper, rubber, plastics, cosmetics, pharmaceutical, and food industries. Because dye wastewater always comes in large quantities, with a complex composition and colour depth, and is of high toxicity, it causes severe environmental pollution and human health hazards if it is not treated properly before discharging into the natural water.

Current treatment methods for dye wastewater include physical, chemical, and biological methods, and so on. Various removal methods have been studied by adsorption,[1–3] chemical catalytic degradation,[4–6] liquid membrane separation,[7] electrolysis,[8] biological treatments,[9] oxidation,[10] and other processes.[11] However, these processes vary in their effectiveness, costs, and environmental impacts.[12] Among these processes, the physical adsorption process and chemical catalytic degradation are much more competitive than other methods for their ready availability, lower cost, and a wider range of applications. It is of vital importance to search for adsorbents which meet the requirements and standards of the water treatment industry and also are environmentally friendly, highly effective, low cost, and being available in tonnage quantities.

In recent years, bio-templating techniques with polysaccharides-based material (cellulose, chitosan, lignin, *etc.*) are actively explored in the fields of metal oxides synthesis due to their environmentally friendly process, facile, required low energy and cost-effective concerns. Cellulose is a natural polysaccharide which has the widest distribution and most abundance on earth. Above all, they can be regenerated. The beads, films, and resins made from natural cellulose were used for heavy metals[13–15] and hazardous azo dyes adsorptions.[16,17] High adsorption enthalpies generated by dyes allow as many aromatic cores to come close to the cellulose surfaces as possible.[18] Furthermore, cellulose is applicable for supporting TiO_2 nanoparticles owing to its good compatibility with TiO_2 nanoparticles. Several types of low-dimensional cellulose materials have been reported, including cellulose nanofibers and films by electrospinning and phase separation method, respectively.[19–23]

However, as compared to other polysaccharides-based materials, cellulose-based materials are the most popular bio-templates used because of their insolubility, which renders them more appropriate for bio-replication than for nanoparticle growth control. For instance, Lu and co-worker had successfully fabricated a millimetre-long TiO_2 fiber with nanostructures using bamboo cellulose fibre as a template. Moreover, cellulose-based material not only can be employed as a bio-template but also to form organic–inorganic hybrid materials with resultant nanomaterials. In the case of zinc oxide (ZnO), bacterial cellulose (BC) membrane was successfully prepared as a host matrix

[a]*State Key Laboratory of Pulp and Paper Engineering, South China University of Technology, Guangzhou 510640, China. E-mail: qihs@scut.edu.cn*

[b]*State Key Laboratory of NBC Protection for Civilian, Beijing, 100191, China. E-mail: larance0130@163.com*

† Electronic supplementary information (ESI) available. See DOI: 10.1039/d0ra04509h

to promote hybridization with Zn^{2+} ions. The resulting nanocomposites exhibited good mechanical properties and high photocatalytic activity in the degradation of methyl orange. Recently, there is increasing attention in the development of visible light-driven TiO_2 photocatalyst.[24–29] This is because the traditional TiO_2 possesses a relatively large band gap, which means that it can only be activated under UV region. This property limits the practical efficiency for solar applications. Currently, there is increasing attention in the doping of TiO_2 with non-metal atoms since it can avoid deteriorating thermal stability of the TiO_2 lattice structure. Titania is one of the most important and widely studied inorganic materials, with a broad range of applications such as pigmenting, gas sensors, corrosion protection, optical coatings, solar cells, and photocatalysis. TiO_2 can be prepared as films, rods, or nanoparticles as required for the desired applications. For the preparation of catalytically active TiO_2 nanoparticles at a larger scale, many methods have been developed, but the only ones of industrial importance are flame pyrolysis and chemical vapour synthesis. Cellulose-based TiO_2 nanocomposite materials, combining the advantages of green support with the photocatalytic properties of the TiO_2, are currently intensely studied for applications in photocatalysis, water purification, or self-cleaning materials.

Graphene oxide (GO), an oxidation product of graphene, is a single sheet from graphite and has the ideal two-dimensional (2D) structure with a monolayer of carbon atoms packed into a honeycomb crystal plane. Considerable attention has been drawn to both graphene and the oxide form over the past several years because of their unique physical and chemical properties and potential applications in various research and industrial fields. Recent studies showed that the graphene oxide is ideal for adsorption of dyes and good for acting as a catalyst carrier substance due to its good mechanical strength and large surface area.[11,30] Therefore, based on the cellulose adsorption properties and the intrinsic properties of graphene oxide, we combined them and introduced TiO_2 to make the removal of dyes more efficient.

In our previous works, we have reported the successful preparation of porous cellulose materials (as films or hydrogels) by dissolving cellulose and dispersing GO in sodium hydroxide/urea/water solution.[31,32] It provides a platform for us to prepare the "dip-catalyst" hydrogels for the removal of methylene blue (MB) dyes. A "dip-catalyst" is accentuated by its great recyclability and convenient deployment, especially due to the fact that its immersion/removal into the reaction media can turn the reaction on/off almost instantaneously. In this work, we aimed to fabricate the green polymer composite aerogel *via* the addition of TiO_2 in the cellulose/GO hydrogels. In the present paper, it is believed that the resultant cellulose/GO hydrogels can be used as an effective bio-template nanoreactor for the dispersion of TiO_2 nanostructures through its three-dimensional porous structures and suitable nanopore size distribution. Although, the cellulose matrix contains GO and TiO_2 nanoparticles, it maintains the hydrogel structure during the catalyst reaction, which will not result in secondary pollution.

2. Experimental

2.1 Materials

The cellulose samples (cotton linters, DP 500) supplied by Hubei Chemical Fiber Group Ltd. (Xiangfan, China) were used. GO dispersion (4 mg ml^{-1}), titanium oxide nanopowder (21 nm, 99.5% trace metals basis) were purchased from Sigma-Aldrich. Sodium hydroxide (NaOH), urea, and other reagents were used as received.

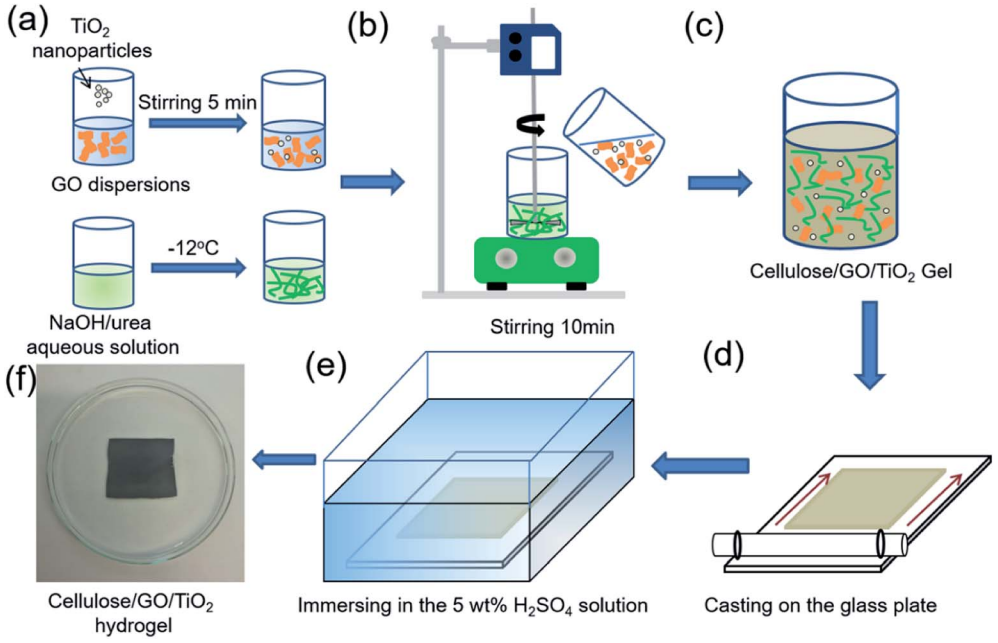

Fig. 1 Fabrication of cellulose/GO/TiO_2 composite hydrogel.

2.2 Preparation of cellulose/GO/TiO_2 hydrogels

Fig. 1 shows the preparation of cellulose/GO/TiO_2 hydrogel. Firstly, the specific amount of TiO_2 nanoparticles was added in 80 ml GO dispersions. A solution of NaOH/urea/H_2O (7 : 12 : 81 by weight) was prepared as the solvent. The designated amounts of NaOH and urea were added into distilled water and then the solvent was pre-cooled to −12 °C. The designated amount of cellulose was added and dissolved into the solvent under vigorous stirring for 5 min to obtain a cellulose solution. Secondly, the GO/TiO_2 solution was added into the cellulose solution under stirring. After degasification, the resulting solution was cast on a glass plate to give a thickness of 500 μm for a gel sheet, and immersed into a coagulation bath with 5 wt% H_2SO_4 for 5 min at room temperature to coagulate and regenerate. The resultant films were washed with running water and deionized water to remove urea and NaOH. Finally, the cellulose/GO/TiO_2 hydrogels consisting of 100 g water, 4 g cellulose, 8 wt% GO and 25 wt% TiO_2 related to the cellulose amount, were obtained.

2.3 Characterization of morphology and microstructure

For the characterization of the composites, the cellulose/GO/TiO_2 hydrogel was rapidly frozen in liquid nitrogen for 5 min and then lyophilized in a freeze drier (Alpha 1-2 LDplus, Christ GmbH, Germany) for 24 h to obtain the of cellulose/GO/TiO_2 aerogel. The scanning electron microscope (SEM) was performed using an Ultra 55 (Carl Zeiss SMT AG, Germany). The prepared aerogel was cryo-fractured in liquid nitrogen for 5 min, and then coated with a thin layer of gold. The samples were prepared by flash freezing after immersion in water, and then sputtered with an approximately 5 nm platinum layer. X-ray diffraction (XRD) was performed using a D/MAX-1200 (Rigaku Co., Japan) with a wavelength of 0.154 nm and a Lynx Eye detector at a scanning rate of $2\theta = 1^\circ$ min^{-1}. Fourier-transform infrared spectroscopy (FTIR) in the range of 4000–500 cm^{-1} was performed on a Spectrum 400 FT-IR/ATR spectrometer (PerkinElmer, USA). X-ray photoelectron spectroscopy (XPS) was performed using an ESCALAB 250 XPS meter with Al Kα monochromatization. Electrochemical impedance spectroscopy (EIS) were carried out on an electrochemical workstation (CHI 660E Chenhua Instrument Company, Shanghai, China) based on a conventional three-electrode system with a frequency range from 0.01 Hz to 100 kHz at the circuit potential.

2.4 Photocatalytic activity evaluation

The photocatalytic activity of cellulose/GO/TiO_2 hydrogel was conducted by the degradation of MB as the model of pollutants in aqueous solution at ambient temperature. Typically, 5 g hydrogel in the shape of a thick film of about 120 × 80 × 0.5 mm^3 were dipped into the 10 mg L^{-1} of MB (200 ml), and stored in the dark place for 60 min to reach adsorption–desorption equilibrium. The solution containing photocatalysts was exposed to the UV irradiation by a 125 W mercury lamp (Vilber Laurmat, $\lambda = 312$ nm) for 1 h and was collected at regular time

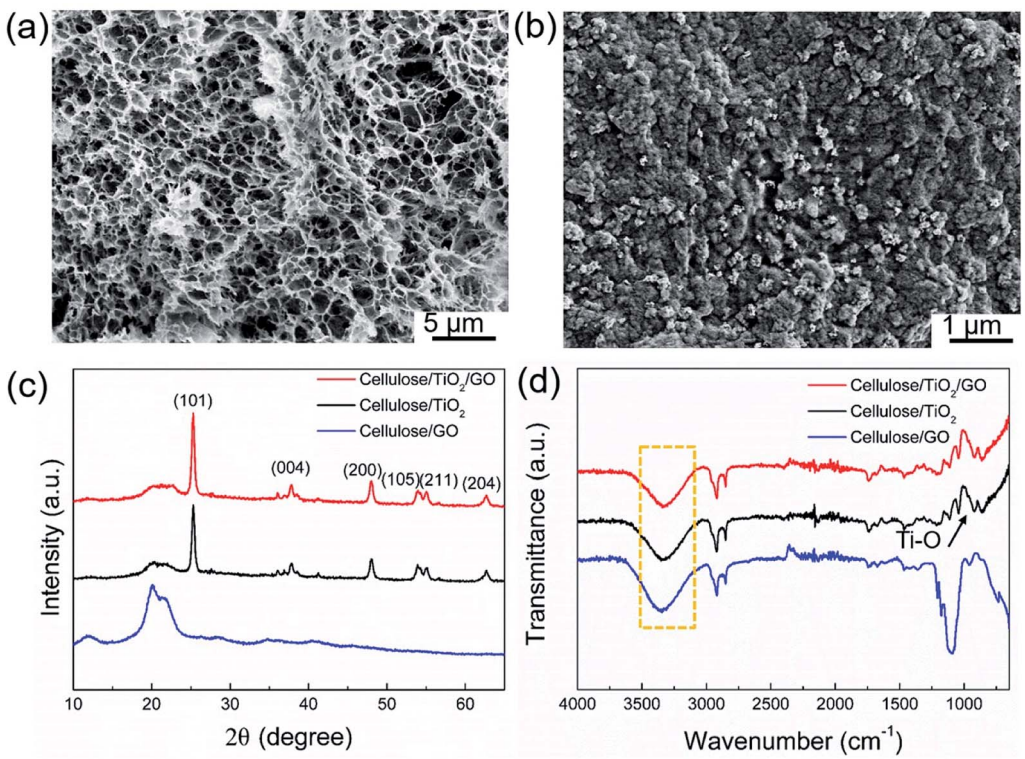

Fig. 2 (a) SEM images of cellulose/GO/TiO_2 aerogel (cross-section) (b) SEM images of cellulose/GO/TiO_2 aerogel (surface); (c) XRD spectrum of cellulose/GO/TiO_2, cellulose/TiO_2, and cellulose/GO; (d) FTIR spectrum of cellulose/GO/TiO_2, cellulose/TiO_2, and cellulose/GO.

intervals during irradiation to evaluate the photocatalytic activity. In order to analysis the effect of absorption of hydrogel on the removal of MB, the solution containing photocatalysts was also under dark condition for 24 h and was also collected at regular time intervals. The concentration of MB was measured by recording its absorbance at 664 nm wavelength with a UV-Vis spectrophotometer (Analytik Jena, Germany) from which the degradation efficiency was calculated. The UV-Vis spectra of the samples were recorded in air atmosphere at room temperature from 200 to 800 nm. The degradation percentages of MB in aqueous solution was calculated as follows: Degradation (%) = $(C_0 - C_t)/C_0 \times 100$, where C_0 is the initial concentration at time $t = 0$, and C_t is the concentration at time interval. For the 10 consecutive cycles, the hydrogel sample was taken from the solution and washed thoroughly with deionized water, and then it was added into fresh MB solution.

3. Results and discussion

3.1 Characterization and analysis of hydrogels

The results of structural and morphological analysis of cellulose/GO/TiO_2 composites are shown in Fig. 2. During the freeze-drying method, water served as a forming agent (more than 90%), was first frozen and then sublimated during the freeze-drying process, leading to the generation of highly 3D porous network structure. Therefore, as shown in Fig. 2a, the cellulose/GO/TiO_2 aerogel own open and highly porous structures with diameters of 300–500 nm. The cellulose hydrogel as the catalyst support provides ideal conditions for the uniform dispersion of TiO_2 nanoparticles and GO sheets, while preserving the structure of the cellulose matrix. The TiO_2 nanoparticles are densely and uniformly coated on the GO sheets and cellulose chains (Fig. 2a and b). The average size of the TiO_2 nanoparticles is about 20–22 nm. It is also worth mentioning that the TiO_2 nanoparticles were directly coated onto the GO surface and cellulose without having any molecular linkers, which is due to the strong hydrogen bonds.

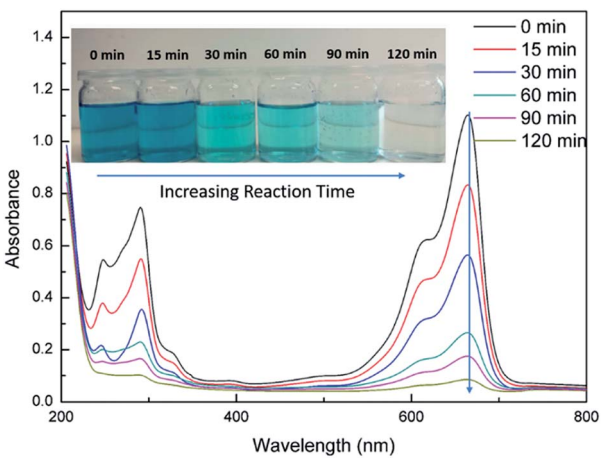

Fig. 3 UV-Vis analysis of the photocatalytic degradation of MB by cellulose/GO/TiO_2 hydrogel with the increasing reaction time.

The crystal structures of cellulose/GO/TiO_2, cellulose/TiO_2, and cellulose/GO composites were further characterized using XRD (Fig. 2c). The peaks at 2θ value of 25.3, 37.8, 48.0, 54.0, 55.1, 62.7, 68.8, 70.3, and 75.1 were indexed to (101), (004), (200), (105), (211), (204), (116), (220), and (215) crystal planes of anatase TiO_2 in cellulose/GO/TiO_2 and cellulose/TiO_2 composite, respectively. XPS spectrum of cellulose/GO/TiO_2, and cellulose/GO were also carried out to study the element composition and chemical states of elements. As shown in Fig. S1a,† the typical photoelectron peaks of C, O and Ti elements confirmed the presence of these three elements. The Ti 2p spectrum of cellulose/GO/TiO_2 and bare TiO_2 shows two symmetrical peaks with binding energies at 459.4 and 465.1 eV, which are attributed to Ti $2p_{3/2}$ and Ti $2p_{1/2}$, respectively (shown in Fig. S1b†).

Fig. 2d shows the FTIR spectrum of cellulose/GO/TiO_2, cellulose/TiO_2, and cellulose/GO. As compared to the cellulose/GO composite, it was observed that O–H stretching absorption peaks in cellulose/GO/TiO_2 composite was slightly shifted from high (3336 cm^{-1}) to low absorption peak (3274 cm^{-1}), and its intensity significantly increased. This could be attributed by the interaction between the O–H groups of cellulose and Ti–O bond of TiO_2. Previous study suggested that this might be due to a strong interaction between the hydroxyl groups of cellulose and the TiO_2 particles through hydrogen bonding interactions.[33] Zhang *et al.*[34] also suggested that it might be due to the partial C–OH occupied by a Ti–O bond. Therefore, it promoted the strong interfacial interaction between cellulose chain and TiO_2 nanoparticles. The strong interfacial interaction increases the durability of the nanoparticles within the nanocomposite membrane and decreases the detachment tendency of the nanofillers in the polymer matrices.[35]

3.2 Photocatalytic analysis of composite hydrogels

In order to study the photocatalytic degradation performance of cellulose/GO/TiO_2 hydrogel, MB was used as a probe pollutant to clarify the removal efficiency of cellulose/GO/TiO_2 hydrogel. Fig. 3 displays that absorptive intensity of MB at 664 nm gradually decreased with the increasing reaction time, when the cellulose/GO/TiO_2 hydrogel was taken into the MB solution under UV light at room temperature. This result indicates that MB underwent degradation behaviour under the catalysis of cellulose/GO/TiO_2 hydrogel. If the degradation ratio is defined as the ratio between the decreased absorptive intensity and that of the initial methylene blue solution, the degradation ratio was about 93% when the mixed solution was irradiated for 120 min. This implies that the prepared cellulose/GO/TiO_2 hydrogel has good photocatalytic activity for MB and are likely to be an efficient photocatalyst.

The removal efficiency of different hydrogels under UV light is presented in Fig. 4a. It can be seen that cellulose and cellulose/GO hydrogels have almost no photoactivity on the removal of MB under UV light. The insignificant removal efficiency of MB was due to the adsorption of MB molecules on the surface of cellulose and GO sheets. These results indicated that the photocatalytic degradation of MB did not occur without

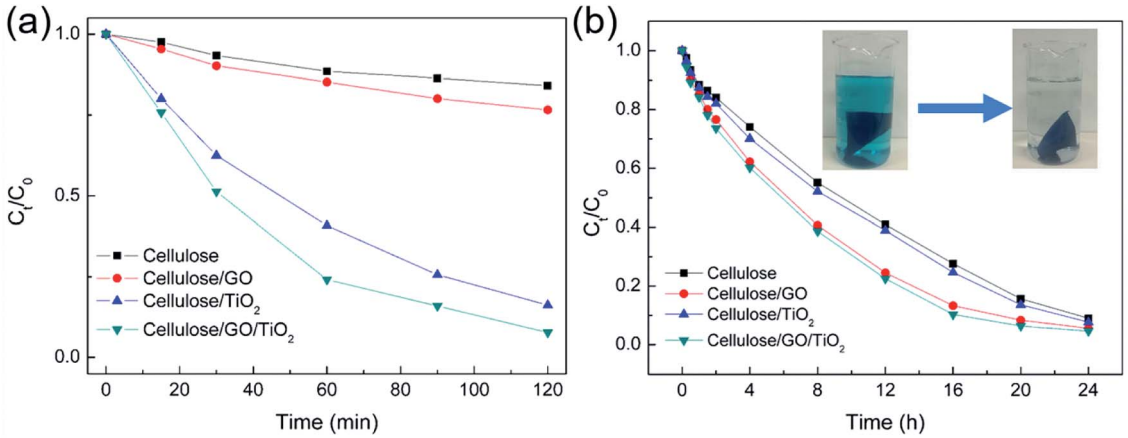

Fig. 4 (a) Photocatalytic degradation rate of MB over the different samples under UV light; (b) absorption rate of MB over the different samples under dark condition.

TiO_2 in the cellulose matrix. While ~93 and ~80% of the initial MB dyes were decomposed by cellulose/GO/TiO_2 and cellulose/TiO_2 hydrogel after 120 min under UV light. The excellent performance in removal efficiency of MB can be attributed to the synergistic effects between GO sheets and TiO_2 and the adsorption of MB molecules on the surface of cellulose and GO sheets. To clarify the absorption effect on the removal efficiency of MB dyes, the adsorption activity of different hydrogels was carried out under dark condition for 24 h. As shown in Fig. 4b, the cellulose/GO/TiO_2 hydrogel was transformed to nattier blue after soaking in the MB solution for 24 h, and many MB molecules remain in the cellulose/GO/TiO_2 hydrogel. Furthermore, the existence of GO sheets could enhance the absorption capacity and therefore, will promote high removal efficiency of MB under the dark condition for 24 h. Furthermore, the cellulose/GO/TiO_2 hydrogel also exhibited higher photoactivity on the removal of MB, compared to bare TiO_2 and GO/TiO_2 system (shown in Fig. S2†).

The reproducible of our cellulose/GO/TiO_2 hydrogel for the photodegradation of MB under UV light and adsorption of MB under dark condition were also carried out in Fig. 5. The photodegradation and adsorption of MB was monitored for ten consecutive cycles, each for 120 min (under UV light) and 24 h (under dark condition), respectively. After each cycle, the cellulose/GO/TiO_2 hydrogel was taken off from MB solution and washed thoroughly with water, then taken into the fresh MB solution. In Fig. 5a, there was no significant decrease in the removal efficiency of MB under UV light during the ten consecutive cycles, indicating the excellent reproducible and durability of the cellulose/GO/TiO_2 hydrogel for the photodegradation of MB. Notedly, in the case of UV light, the photodegradation of MB which is due to the synergetic effect between TiO_2 and GO played a major role in the removal of MB. The introduction of GO sheets probably brought in an intermediate energy level above the valence band of TiO_2, thereby narrowing the band-gap to induce UV light absorption. Therefore, the high and stable performance of the cellulose/GO/TiO_2 hydrogel for the photodegradation of MB should be attributed to the co-effect of between TiO_2 and GO. Moreover, with the unique porous structure of cellulose hydrogel and two-

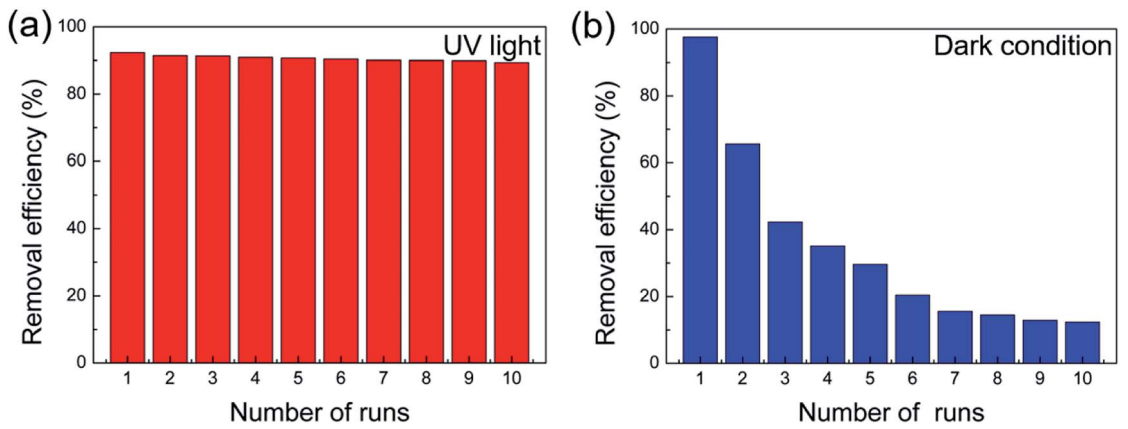

Fig. 5 (a) The long-term stability of photocatalytic degradation of cellulose/GO/TiO_2 hydrogel was tested by repeated use for MB under UV light; (b) the long-term stability of absorption performance of cellulose/GO/TiO_2 hydrogel was tested by repeated use for MB under dark condition.

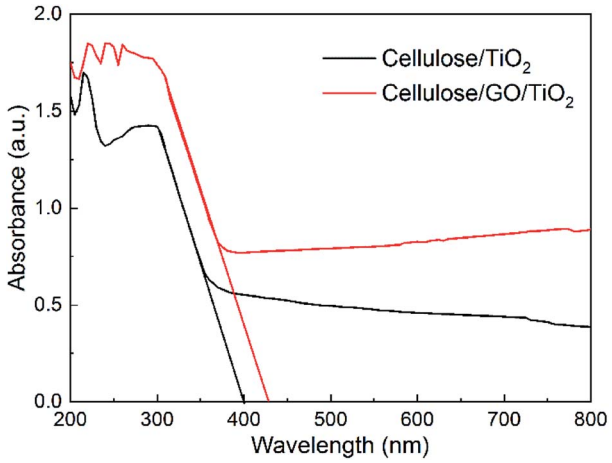

Fig. 6 Diffuse reflectance absorption spectra of cellulose/TiO_2 and cellulose/GO/TiO_2 hydrogel.

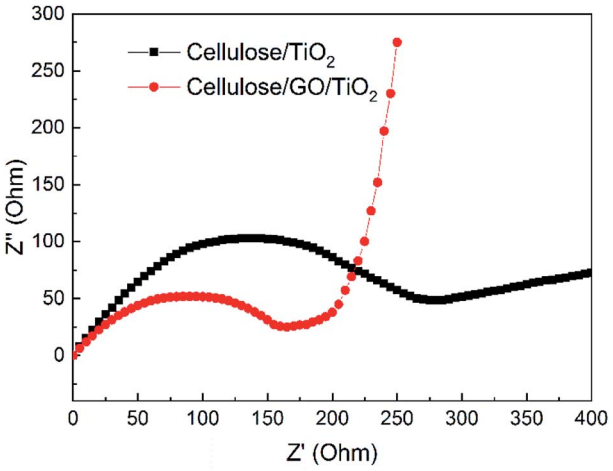

Fig. 7 Electrochemical impedance spectroscopy (EIS) Nyquist plots of cellulose/TiO_2 and cellulose/GO/TiO_2 hydrogel.

dimensional planar structure of GO, the enhanced absorptivity of cellulose/GO/TiO_2 hydrogel also promoted the high and stable performance of this hydrogel.

Conversely, there was an obvious decrease in the removal efficiency of MB under dark condition in Fig. 5b. In the case of dark condition, the removal of MB is ascribed to the absorption of MB on the surface of cellulose and GO due to the porous structure of hydrogel. As shown in Fig. 5b, there is an obvious change in the cellulose/GO/TiO_2 hydrogel after the first absorption run. Although the hydrogel was washed thoroughly with water before the next run, many MB molecules remain in the cellulose/GO/TiO_2 hydrogel, leading to the weakening of the next absorption effect of this hydrogel.

In addition, light absorption plays an important role in the photodegradation of MB. Fig. 6 shows the electronic absorption spectra of cellulose/TiO_2 and cellulose/GO/TiO_2 hydrogel. There is a clear red shift in the absorption edge of cellulose/GO/TiO_2 hydrogel, compared to cellulose/TiO_2 hydrogel. This result can be attributed to the interaction between GO and TiO_2. The introduction of GO sheets probably brought in an intermediate energy level above the valence band of TiO_2, thereby narrowing the band-gap to induce UV light absorption. This narrowing is also beneficial for a more efficient utilization of light in the removal of MB.

Charge transfer efficiency is another important factor during the photocatalysis process. As shown in Fig. 7, the typical electrochemical impedance spectra of cellulose/TiO_2 and cellulose/GO/TiO_2 hydrogel were presented as Nyquist plots, and it is observed that, arc radius on the plot of cellulose/GO/TiO_2 hydrogel is smaller than that of cellulose/TiO_2 hydrogel, which indicated the higher efficiency of charge separation. GO here acted as an electron acceptor and inhibited electron–hole recombination, and the strong coupling between TiO_2 and GO facilitated interfacial charge transfer.

Overall, cellulose/GO/TiO_2 hydrogel was prepared by a simple, green and one-step process. Owing to its unique porous structure and introduction of GO, cellulose/GO/TiO_2 hydrogel showed superior and reproducible performance in the removal of MB under UV light. Therefore, the schematic representation of photocatalytic degradation and absorption mechanism of cellulose/GO/TiO_2 hydrogel for MB under UV light was proposed (Fig. 8). The enhanced photocatalytic and adsorption performance for the cellulose/GO/TiO_2 hydrogel can be ascribed to their unique structure with the following favourable properties: (i) the porous structure of cellulose hydrogel with a relatively high surface area can provide more active sites and increase surface adsorption of reactant species on the surface of composite photocatalysts; (ii) the conjugated MB molecules could bind to large aromatic domains on GO sheets *via* π–π stacking, which could favour increased reactivity[36] and effectively improve the light absorption in the visible region; (iii) the high photocatalytic and reproducible performance of our hydrogel could also be a result of the strong coupling between TiO_2 and GO which facilitates interfacial charge transfer (with GO as an electron acceptor) and inhibits electron–hole recombination.[37]

In order to have a rough estimation of the removal efficiency of cellulose/GO/TiO_2 hydrogel as the catalyst to degrade MB, the degradation performance and stability were compared with those reported in the literature. Table 1 contains different catalysts able to degrade MB dye at similar operational conditions. Under this condition, most of the recent reports have lower removal percentage of MB than the here reported ones. Compared to them, the cellulose/GO/TiO_2 hydrogel exhibited good degradation performance and excellent recyclability. Moreover, another advantage of the hydrogel as the catalyst is that the cellulose matrix contains GO and TiO_2 nanoparticles and maintains the hydrogel structure during the catalyst reaction, which will not result in secondary pollution. The "dip-catalyst" can be easily removed from the polluted water after the degradation reaction. In other words, it is easy to start and stop the degradation reaction by taking in and out the whole hydrogel. It is obvious that the cellulose/GO/TiO_2 hydrogel, with its sustainable feature, convenient fabrication, great catalytic

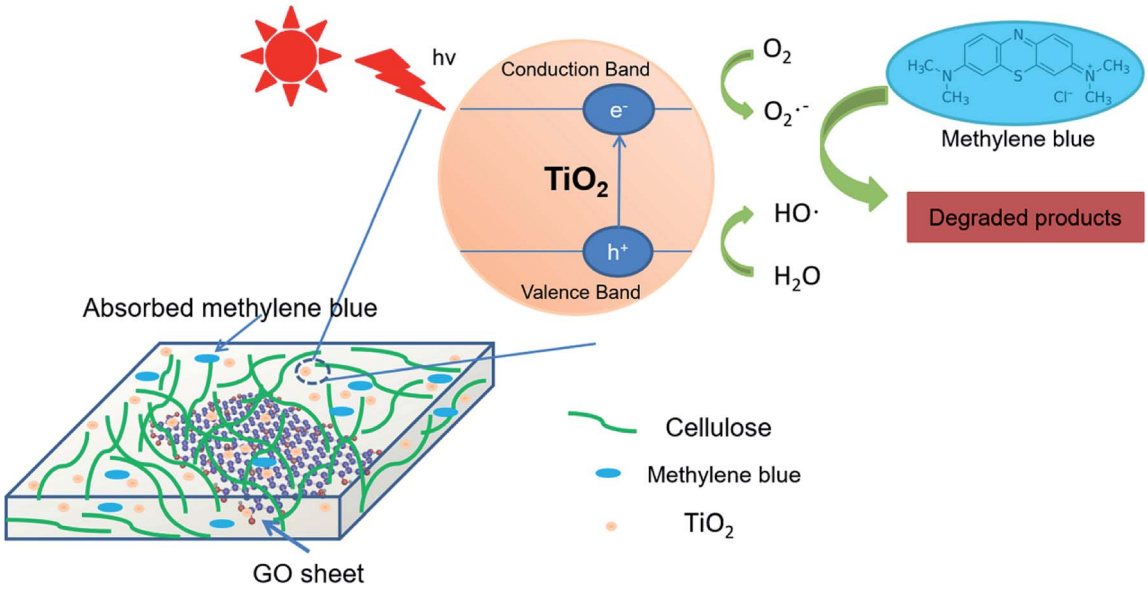

Fig. 8 The schematic representation of photocatalytic degradation and absorption mechanism of cellulose/GO/TiO_2 hydrogel for MB under UV light.

Table 1 Photocatalytic degradation activity of MB over different systems under UV light

Sample	Removal efficiency	Reaction time (min)	Reproducible	Ref.
Cellulose/TiO_2 films	75%	60	5	38
Polymer nanofibers/TiO_2	70%	180	4	22
Niobium oxyhydroxide dispersed poly(3-hydroxybutyrate) films	92%	120	7	39
Cellulose/GO/TiO_2 hydrogel	93%	120	10	This work

efficiency, good recyclability, and easy removability is expected to be very useful in MB dyes removal.

4. Conclusions

In summary, environmentally friendly cellulose/GO/TiO_2 hydrogel photocatalyst has been successfully fabricated *via* a green, simple, and one-step method and evaluated as the photocatalyst and adsorbent for the removal of MB. The XRD and FTIR analysis suggested the strong interaction among cellulose, GO and TiO_2, resulting from the formation of hydrogen bonds. Due to the unique porous structure of cellulose hydrogel and introduction of GO, the cellulose/GO/TiO_2 hydrogel showed superior (degradation ratio $\sim$ 93%) and reproducible (no significant during the ten consecutive cycles) performance in the removal of MB under UV light. Consequently, the prepared cellulose/GO/TiO_2 hydrogel can be applied as eco-friendly, high-performance, reproducible, and stable photocatalyst and adsorbent for the removal of MB. This green hydrogel is a promising candidate for dye wastewater treatment. Moreover, this work is expected to extend the scope of bio-templated synthesis of other nanomaterials for various applications.

Conflicts of interest

There are no conflicts to declare.

Acknowledgements

The authors are grateful for the financial support for this work by the National Natural Science Foundation of China (21774036), Guangdong Province Science Foundation (2017B090903003, 2017GC010429).

Notes and references

1 X. Liang, P. Wang, M. Li, Q. Zhang, Z. Wang, Y. Dai, X. Zhang, Y. Liu, M.-H. Whangbo and B. Huang, *Appl. Catal., B*, 2018, **220**, 356–361.
2 Y. Zhang, W. Cui, W. An, L. Liu, Y. Liang and Y. Zhu, *Appl. Catal., B*, 2018, **221**, 36–46.
3 J. Cunningham, G. Al-Sayyed and S. Srijaranai, in *Aquatic and surface photochemistry*, CRC Press, 2018, pp. 317–348.
4 K. He, G. Chen, G. Zeng, A. Chen, Z. Huang, J. Shi, T. Huang, M. Peng and L. Hu, *Appl. Catal., B*, 2018, **228**, 19–28.

5 P. Xiao, P. Wang, H. Li, Q. Li, Y. Shi, X.-L. Wu, H. Lin, J. Chen and X. Wang, *J. Hazard. Mater.*, 2018, **345**, 123–130.
6 J. Kang, H. Zhang, X. Duan, H. Sun, X. Tan, S. Liu and S. Wang, *Chem. Eng. J.*, 2019, **362**, 251–261.
7 A. Dâas and O. Hamdaoui, *J. Hazard. Mater.*, 2010, **178**, 973–981.
8 L. Wang, *J. Hazard. Mater.*, 2009, **171**, 577–581.
9 M. H. El-Naas, S. A. Al-Muhtaseb and S. Makhlouf, *J. Hazard. Mater.*, 2009, **164**, 720–725.
10 H. T. Gomes, B. F. Machado, A. Ribeiro, I. Moreira, M. Rosário, A. M. Silva, J. L. Figueiredo and J. L. Faria, *J. Hazard. Mater.*, 2008, **159**, 420–426.
11 T. Wu, X. Cai, S. Tan, H. Li, J. Liu and W. Yang, *Chem. Eng. J.*, 2011, **173**, 144–149.
12 S. Chakraborty, M. Purkait, S. DasGupta, S. De and J. Basu, *Sep. Purif. Technol.*, 2003, **31**, 141–151.
13 S. Allen, G. Mckay and J. F. Porter, *J. Colloid Interface Sci.*, 2004, **280**, 322–333.
14 K. Z. Elwakeel, *J. Hazard. Mater.*, 2009, **167**, 383–392.
15 G. Crini and P.-M. Badot, *Prog. Polym. Sci.*, 2008, **33**, 399–447.
16 S. J. Allen, Q. Gan, R. Matthews and P. A. Johnson, *Ind. Eng. Chem. Res.*, 2005, **44**, 1942–1949.
17 G. Annadurai, R.-S. Juang and D.-J. Lee, *J. Hazard. Mater.*, 2002, **92**, 263–274.
18 J. Bird, N. Brough, S. Dixon and S. N. Batchelor, *J. Phys. Chem. B*, 2006, **110**, 19557–19561.
19 X. Jin, J. Xu, X. Wang, Z. Xie, Z. Liu, B. Liang, D. Chen and G. Shen, *RSC Adv.*, 2014, **4**, 12640–12648.
20 A. Wittmar, D. Vorat and M. Ulbricht, *RSC Adv.*, 2015, **5**, 88070–88078.
21 A. W. Morawski, E. Kusiak-Nejman, J. Przepiórski, R. Kordala and J. Pernak, *Cellulose*, 2013, **20**, 1293–1300.
22 A. Abdal-hay, A. S. Hamdy Makhlouf and K. A. Khalil, *ACS Appl. Mater. Interfaces*, 2015, **7**, 13329–13341.
23 A. Wittmar, H. Thierfeld, S. Köcher and M. Ulbricht, *RSC Adv.*, 2015, **5**, 35866–35873.
24 X. Zhu, H. Xu, Y. Yao, H. Liu, J. Wang, Y. Pu, W. Feng and S. Chen, *RSC Adv.*, 2019, **9**, 40003–40012.
25 L. Pan, M. Ai, C. Huang, L. Yin, X. Liu, R. Zhang, S. Wang, Z. Jiang, X. Zhang, J. Zou and W. Mi, *Nat. Commun.*, 2020, **11**, 418.
26 H. Li, P. Wang, X. Yi and H. Yu, *Appl. Catal., B*, 2020, **264**, 118504.
27 Y. Wang, G. Shen, Y. Zhang, L. Pan, X. Zhang and J. Zou, *Appl. Catal., B*, 2020, **260**, 118183.
28 D. Gao, W. Liu, Y. Xu, P. Wang, J. Fan and H. Yu, *Appl. Catal., B*, 2020, **260**, 118190.
29 A. Jian, M. Wang, L. Wang, B. Zhang, S. Sang and X. Zhang, *RSC Adv.*, 2019, **9**, 41540.
30 G. Ramesha, A. V. Kumara, H. Muralidhara and S. Sampath, *J. Colloid Interface Sci.*, 2011, **361**, 270–277.
31 Y. Chen, P. Pötschke, J. Pionteck, B. Voit and H. Qi, *J. Mater. Chem. A*, 2018, **6**, 7777–7785.
32 Y. Chen, P. Pötschke, J. r. Pionteck, B. Voit and H. Qi, *ACS Omega*, 2019, **4**, 5117–5125.
33 S. X. Shu and C. R. Li, *Adv. Mater. Res.*, 2012, **418**, 237–241.
34 X. Zhang, W. Chen, Z. Lin, J. Yao and S. Tan, *Synth. React. Inorg., Met.-Org., Nano-Met. Chem.*, 2011, **41**, 997–1004.
35 P. Goh, B. Ng, W. Lau and A. Ismail, *Sep. Purif. Rev.*, 2015, **44**, 216–249.
36 D. Ravelli, D. Dondi, M. Fagnoni and A. Albini, *Chem. Soc. Rev.*, 2009, **38**, 1999–2011.
37 W. Wang, P. Serp, P. Kalck and J. L. Faria, *Appl. Catal., B*, 2005, **56**, 305–312.
38 A. Snyder, Z. Bo, R. Moon, J.-C. Rochet and L. Stanciu, *J. Colloid Interface Sci.*, 2013, **399**, 92–98.
39 A. P. Heitmann, P. S. Patrício, I. R. Coura, E. F. Pedroso, P. P. Souza, H. S. Mansur, A. Mansur and L. C. Oliveira, *Appl. Catal., B*, 2016, **189**, 141–150.